Polymer 60 (2015) 198–206

Contents lists available at ScienceDirect

Polymer

journal homepage: www.elsevier.com/locate/polymer

Processing and performance of aromatic-aliphatic thermotropic polyesters based on vanillic acid

Carolus H.R.M. Wilsens [a, b, c], Yogesh S. Deshmukh [c], Wenqing Liu [d], Bart A.J. Noordover [a], Yefeng Yao [d], Han E.H. Meijer [a], Sanjay Rastogi [b, c, e, *]

[a] Laboratory of Polymer Materials, Eindhoven University of Technology, Den Dolech 2, 5600MB Eindhoven, The Netherlands
[b] Dutch Polymer Institute (DPI), P.O. Box 902, 5600AX Eindhoven, The Netherlands
[c] Department of Biobased Materials, Maastricht University, P.O. Box 616, 6200MD Maastricht, The Netherlands
[d] Shanghai Key Laboratory of Magnetic Resonance, East China Normal University, North Zhongshan Road 3663, 200062 Shanghai, PR China
[e] Department of Materials, Loughborough University, England, UK

ARTICLE INFO

Article history:
Received 13 November 2014
Received in revised form
15 January 2015
Accepted 19 January 2015
Available online 26 January 2015

Keywords:
Fiber
Thermotropic melt
Vanillic acid

ABSTRACT

In this work we report on the processing, melt-drawing, and performance of new vanillic acid based aliphatic-aromatic thermotropic polyesters. It is demonstrated that these materials are easily processed from their nematic melts yielding highly oriented products. Furthermore, we demonstrate that a molecular weight (M_w) of roughly 30 kg/mol is required in order to successfully perform spinning on these polymers. The application of a polymer with lower M_w results in poor mechanical performance and fiber breakage during the winding process. Wide-angle X-ray diffraction analysis has been performed on the fibers and it is demonstrated that the orientation parameter increases with increasing draw-ratio of the fiber. Although these polymers are readily processed from their thermotropic melts, the obtained fibers only retain their orientation up to temperatures in the range of 120–130 °C, after which they start to melt. In general, these fibers exhibit tensile moduli in the range of ~10 GPa and a tensile strength around ~150–200 MPa. FTIR and solid-state NMR experiments indicate that only the aromatic components are molecularly oriented during the spinning process. In contrast, the aliphatic moieties exhibit a high mobility, normally corresponding to a local isotropic motion. It is expected that the poor molecular orientation of the aliphatic moieties in these aliphatic-aromatic thermotropic polyesters contribute to the relatively low tensile modulus of the fibers, obtained after the extrusion and melt-drawing process.

1. Introduction

The synthesis, processing and performance of thermotropic polyesters have widely been investigated over the last decades. Their low melt-viscosity, the ease in processing and the highly anisotropic products obtained after melt-processing have resulted in numerous publications and commercialization of different thermotropic polyesters [1–8]. Perhaps the most widely used thermotropic polyesters are the *p*-hydroxybenzoic acid (BA) and 6-hydroxy-2-naphthoic acid (NA) based copolymers, commercially known as the Vectra® series. Generally, fibers spun from the Vectra® polymer series (Vectran® fibers), have tensile moduli around 50 GPa and tensile strengths of over 1 GPa after processing from their thermotropic melt. Additionally, heat treatment of these fibers increases their mechanical performance, yielding fibers with tensile moduli ~100 GPa and tensile strengths around 3–4 GPa. Generally, the increase in tensile modulus upon heat-treatment is attributed to the reorganization of the monomer sequences resulting in the formation of bigger and more perfect crystals. The improved tenacity of the fibers after heat-treatment is attributed to the occurrence of a post-condensation reaction, resulting in an increase of the molecular weight which facilitates a better stress transfer along the polymer chains [9].

From this data it becomes clear that heat-treatment is essential for semi-crystalline fully aromatic thermotropic polyester fibers, to achieve the best mechanical performance. However, the application of such a heat-treatment is only possible when the obtained fiber is dimensionally stable at the applied annealing temperatures,

* Corresponding author. Dutch Polymer Institute (DPI), P.O. Box 902, 5600AX Eindhoven, The Netherlands.
E-mail addresses: s.rastogi@lboro.ac.uk, sanjay.rastogi@maastrichtuniversity.nl (S. Rastogi).

http://dx.doi.org/10.1016/j.polymer.2015.01.045
0032-3861/

commonly in the range of 250–300 °C. For example, the application of such a heat-treatment is not possible for amorphous thermotropic polyesters or for thermotropic polyesters that have too low melting temperatures. An example of an amorphous fully aromatic thermotropic polyester, based on terephthalic acid, NA, and 4,4′-dihydroxy-2,2′-dimethyl-biphenyl, has been reported by Grasser and coworkers [10]. Although these polymers exhibited no melting or crystallization transition, fiber spinning from the thermotropic melt yielded fibers with tensile modulus in the range of 50 GPa and a tensile strength of approximately 0.5 GPa.

A well-known example of aliphatic-aromatic thermotropic polyesters is the copolymer of poly(ethylene terephthalate) (PET) and BA. Depending on the processing temperature, processing of these copolymers with 60 mol% BA from the thermotropic melt yields fibers having tensile moduli between 10 and 30 GPa [11,12]. Another example of thermotropic fibers spun from aliphatic-aromatic polymers has been reported by Dingemans and coworkers [13]. These authors reported the synthesis and preliminary fiber spinning results of polymers containing flexible suberic acid and sebacic acid spacers. The obtained fibers exhibit a tensile modulus of 15 GPa and a tensile strength of 0.12 GPa. Although the presence of these aliphatic spacers drastically decreases the tensile performance of the obtained fibers, it is clear that fibers with promising tensile moduli can still be obtained. Besides, these aliphatic spacers drastically decrease the melting and processing temperatures of thermotropic polymers, and allow for the incorporation of monomers that are thermally instable at high temperatures.

In previous publications, we have reported routes to successfully design thermotropic polyesters based on vanillic acid (Fig. 1) [14,15]. In these publications we demonstrated that the synthesis of high molecular weight copolymers containing small amounts of vanillic acid could be performed at low temperatures from the melt, generally yielding polymers with melting temperatures close to or below 200 °C. Furthermore, the presence of vanillic acid is known to (a) improve the monomer sequence distribution, (b) increase the stability of the thermotropic melt, (c) decrease the polymer melting temperature, and (d) improve the spinnability of thermotropic polyesters [15–18]. To be more specific and relevant for the polymers investigated in this publication (Fig. 1) is that the presence of vanillic acid results in a crystal to nematic (K–N) phase transition close to 150 °C. No nematic to isotropic (N–I) transition was observed prior to degradation. Thus the preferred processing window for these polymers exists above 150 °C. Although the benefits of the copolymerization of vanillic acid are interesting from a chemical viewpoint, the low melting temperature of the polymers limits the application of these polymers at high temperature and might not allow for the processed products to undergo a heat-treatment step. These factors, mainly resulting from the presence of the aliphatic spacers, might limit the application of these fibers for practical purposes.

In this manuscript we evaluate the effect of different processing routes on the mechanical performance of vanillic acid based renewable aliphatic-aromatic thermotropic polyesters having different molecular weights. The used processing conditions are fiber spinning, compression molding, and solvent casting. Differential scanning calorimetry (DSC), dynamic mechanical thermal analysis (DMTA), wide-angle x-ray diffraction (WAXD), polarization optical microscopy (POM), Fourier-Transform Infra-Red (FTIR), and solid-state NMR spectroscopy are used to characterize the processed products. Special attention is paid to the thermal behavior, orientation and mechanical performance of the processed products and possibilities to perform heat-treatment steps are investigated.

2. Experimental section

2.1. General polymerization procedure

Thermotropic polyesters containing *p*-hydroxybenzoic acid (HBA), vanillic acid (VA), suberic acid (SuA), and hydroquinone (HQ) were prepared using a 200 g scale acidolysis melt-polycondensation reaction. The monomers were loaded into a 500 mL three-neck round bottom flask fitted with a mechanical stirrer, together with 50–100 mg of $Zn(AcO)_2$ and the temperature was gradually increased to 260 °C. Acetic acid was distilled off and reduced pressure was applied to the system for eight to twelve hours after roughly 90% of the expected acetic acid was collected. Details regarding the polymerization procedure are reported in a previous publication [15].

2.2. Processing of thermotropic polyesters

Solvent cast films of the polymers used in this study were prepared via dissolution of polymer samples in a 2:1 mixture (v/v) of chloroform/1,1,1,3,3,3-hexafluoroisopropanol ($CHCl_3$/HFIP) at room temperature. The concentrations of the casting solutions were 1 g polymer per 3 mL solvent. Once the polymers were fully dissolved, the casting solutions were poured onto an aluminum plate and the films were allowed to dry at room temperature for 3 h followed by drying *in vacuo* at 40 °C overnight. The obtained polymer films were slightly yellow/brown and transparent. To ensure the full removal of any residual solvent, heat treatment and thorough drying of the samples was performed in a second drying step above T_g at 80 °C.

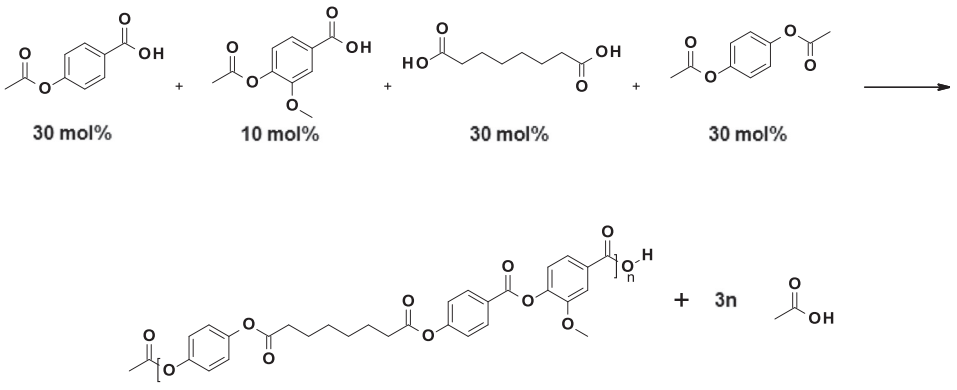

Fig. 1. Acidolysis reaction and composition of polymers **I**–**III** synthesized in this study. *N.b.* the resulting polymer is a copolymer.

Compression molding of the polymers was performed using a P 300 E Collins compression mold. Samples were compression molded in shapes of 30 mm × 40 mm × 0.5 mm at 10 °C above their melting temperature as observed in DSC analysis.

Small scale extrusion and melt drawing experiments were performed using a DSM Xplore MC15 twin-screw extruder. Prior to the processing, the polymers were dried *in vacuo* overnight at 80 °C. The dried polymer was loaded into a mini-extruder via a water-cooled hopper under a nitrogen rich flow to prevent degradation or depolymerization. Samples were mixed and extruded at a screw rotation speed of 50 rpm at 10 °C above their melting temperatures. The extrudate was quenched in a water bath located 1 cm from the extruder outlet and was wound on a bobbin having a diameter of 10 cm. The extrudate was spun at different winding speeds to obtain fibers having different draw ratios. The obtained fibers were dried *in vacuo* for 48 h at room temperature prior to any measurement.

2.3. Characterization methods

Molecular weights and polydispersity index (PDI) values were determined *via* 1,1,1,3,3,3-hexafluoroisopropanol (HFIP) size exclusion chromatography (SEC). This system is equipped with a Waters 1515 Isocratic HPLC pump, a Waters 2414 refractive index detector (40 °C), a Waters 2707 autosampler, and a PSS PFG guard column followed by 2 PFG-linear-XL (7 mm, 8 × 300 mm) columns in series at 40 °C. HFIP (Apollo Scientific Limited) with potassium trifluoroacetate (3 g L^{-1}) was used as an eluent at a flow rate of 0.8 mL min^{-1}. The molecular weights were calculated against poly(methyl methacrylate) standards (Polymer Laboratories, M_p = 580 Da up to $M_p = 7.1 \times 10^6$ Da). SEC samples were filtered through a 200 μm filter prior to injection.

The thermal stability of the polymers was determined using thermogravimetric analysis (TGA), which was performed on a TA Instruments TGA Q500 in a nitrogen rich atmosphere. Samples were heated at 20 °C/min from 20 °C to 800 °C.

The glass transition temperature (T_g) and the peak transition temperature from the crystalline to the LC phase (T_m) were determined by differential scanning calorimetry (DSC) using a TA Instruments Q1000 DSC. The normal heating and cooling-rates of the samples were 10 °C/min and measurements were performed under a nitrogen rich atmosphere.

Dynamic mechanical thermal analysis (DMTA) was performed on a TA Instruments DMA Q800. DMTA samples were prepared via compression molding at temperatures between 220 °C and 260 °C and were cut into rectangular shapes of 20 mm × 5 mm × 0.5 mm. All experiments were performed at a frequency of 1 Hz and at a heating rate of 2 °C/min. Measurements were continued until the sample was molten or broken. The T_g values determined from DMTA analysis were obtained by taking the maximum value of the loss modulus during heating. DMTA experiments on the fibers were performed after cutting them into strands of 25 mm.

Tensile test experiments were performed at a constant deformation rate of 5 mm/min using a Zwick 100 tensile apparatus and a load cell of 100 N at room temperature. Samples were prepared via compression molding and cut into dog-bone shaped samples of 20 mm × 2 mm × 1 mm. The spun fibers were loaded in the clamps after pasting the fiber ends on a 3 M sticky note, to ensure fiber breakage occurred in the center of the fiber and not in the clamped section. Measurements resulting in fiber breakage at the clamp position were discarded to ensure repeatability of the tensile tests.

Morphologies of the synthesized polymers were determined on a Zeiss Axioplan 2 Imaging optical microscope under crossed polarizers and CD achorplan objectives (32 × zoom). A THMS 600 heating stage connected to a Linkam TMS 94 control unit was mounted onto the optical microscope. Samples were prepared by placing a small amount of ground polymer in-between two glass slides. Optical micrographs were taken at various temperatures, while heating at a rate of 10 °C/min.

Rheological experiments performed in the thermotropic melt were conducted using a TA Instruments ARG2 rheometer. Parallel plate geometry of a diameter of 25 mm and a thickness of 1 mm was used to identify the rheological response of the thermotropic melt. Experiments were performed in the linear viscoelastic regime at a fixed strain of 1.25%. Frequency sweeps were performed in the temperature range between 150 °C and 320 °C. Prior to the data collection points, the samples were allowed to relax for 15 min at the starting temperature of the experiments.

2D fiber patterns were obtained with a Bruker D8 equipped with GADDS, a 2-dimensional detector system using CuK_α radiation, wavelength 1.54184 Å, obtained at 40 kV and 40 mA. A parabolic Göbel mirror is used to provide a highly parallel beam whereby the Kβ and Bremsstrahlung effect is suppressed. The measurements were performed in transmission mode with a sample to detector distance of 50 mm and an exposure time of 30 min. The orientation parameter $<P_{2n}(\cos\varphi)>_d$ was calculated via the procedure described by Mitchell and Windle [19]. The azimuthal intensity $I(\varphi)$ at the maximum of the inter-chain diffraction peak ($2\theta = 21°$) was taken. The orientation parameter $<P_{2n}(\cos\varphi)>_d$ was then determined from an average of a Legendre polynomial, weighted against the obtained azimuthal intensity scan using equations (1)–(3). In this case, only the second order Legendre polynomial was taken into account, yielding $<P_{2n}(\cos\varphi)>_m = -0.5$.

$$<P_{2n}(\cos\varphi)>_d = \frac{<P_{2n}(\cos\varphi)>}{<P_{2n}(\cos\varphi)>_m} \tag{1}$$

$$<P_{2n}(\cos\varphi)> = \frac{\int_0^{\pi/2} I(\theta,\varphi)P_{2n}(\cos\varphi)\sin\varphi\,\delta\varphi}{\int_0^{\pi/2} I(\theta,\varphi)\sin\varphi\,\delta\varphi} \tag{2}$$

$$<P_{2n}(\cos\varphi)>_m = \frac{(2n)!}{(-1)^n 2^{2n}(n!)^2} = -\frac{1}{2} \text{ for the second term} \tag{3}$$

The obtained order parameter reflects the contributions of the distribution of the director orientation throughout the bulk polydomain sample and the contributions of the director on a molecular level [20]. In short, the orientation parameter reflects the degree of anisotropy of the scattering of polymer chains, while assuming that these chains are infinitely long rigid rods. The values of S vary from 0, corresponding to a random chain orientation similar to the orientation of an isotropic liquid, to unity, corresponding to the perfect alignment of the polymer chains along the orientational axis.

3. Results and discussion

3.1. Synthesis and characterization of thermotropic polyesters

Thermotropic polyesters containing 30 mol% p-hydroxybenzoic acid, 30 mol% suberic acid, 30 mol% 1,4-dihydroxybenzene, and 10 mol% vanillic acid (Fig. 1) were synthesized following the general polymerization procedure described in the experimental section. The copolymerization of 10 mol% vanillic acid was performed to ensure a random incorporation of the monomers along the polymer backbone and to reduce the melting temperature of the polymer. To identify the effect of the molecular weight on the processing of this

type of thermotropic polyesters, three batches (**I**–**III**) were synthesized with increasing molecular weights. The molecular weight of the final polymer was controlled by increasing the reaction time; to illustrate, polymer **I** was allowed to build up molecular weight for 4 h, polymer **II** for 8 h, and polymer **III** for 12 h. The polymers were isolated from the melt and were directly used for fiber spinning, compression molding or solvent casting without further purification or heat-treatment step. Table 1 shows an overview of the molecular weights, thermal transitions, and tensile performance after compression molding of polymers **I**–**III**.

As is shown in Table 1, the weight average molecular weight (M_w) of polymers **I**, **II**, and **III** are 17.3 kg/mol, 31.2 kg/mol and 43.8 kg/mol, respectively. According to both DSC and DMTA analysis, the glass transition temperature (T_g) of these polymers increases slightly with increasing molecular weight. This increase of the T_g is likely a result from the decrease of the number of end-groups with increasing molecular weight. Similar to the T_g, the transition from crystal to the nematic phase (T_m) of these polymers increases slightly with increasing molecular weights. It should be noted that none of the polymers **I**–**III** exhibit a nematic to isotropic transition (N–I) upon heating, while heating in hot-stage polarization optical microscopy [15].

The tensile modulus (E) and the maximum tensile stress (σ_{max}) of the compression molded products do not seem to be strongly influenced by the molecular weight of the polymers **I**–**III** (Fig. 2). It should be noted that the σ_{max} and E modulus of polymer **II** is slightly lower than polymer **I**; the subtle differences can be attributed to higher crystallinity expected in the low molar mass polymer **I** compared to polymer **II**. The higher crystallinity of polymer **I** can be a result of the extended chains participating in the domain of only one crystal. However, with the increasing molar mass, as the chains traverse from one to other crystal domains, the resistance to uniaxial deformation is likely to increase causing an increase in modulus and strain to break (as is the case of polymers **II** and **III**). The increase in strain-to-break is in agreement with the expected decrease in the end groups with increasing molar mass. From Fig. 2, the strain at break (ε_{break}) does increase with increasing molecular weight, but no strain hardening during uniaxial deformation is observed for polymers **I**–**III**. The absence of strain-hardening during deformation suggests that these liquid crystalline polymers are not or only loosely entangled.

The viscoelastic response of polymer **III**, having the highest M_w of the three polymers was investigated as a function of frequency at different temperatures (Fig. 3). Prior to the evaluation of the data, the authors would like to note that caution should be taken when interpreting this rheological data; Rheology on rigid liquid crystalline polyesters that have an inaccessible isotropic phase is generally complex due to the inability to remove the thermal and flow history of the sample [21]. Besides, continuous transesterification occurs in the polyester melt, possibly influencing the chemical microstructure of copolymers and thus changing the rheological response. These factors limit the repeatability of rheological experiments of thermotropic polyesters. In order to minimize errors from thermal and flow history, all samples were cut into discs with a diameter of 25 mm from the same compression molded sheet having a thickness of 1 mm. Furthermore, the samples were allowed to equilibrate for 15 min at the desired temperature prior to the experiment.

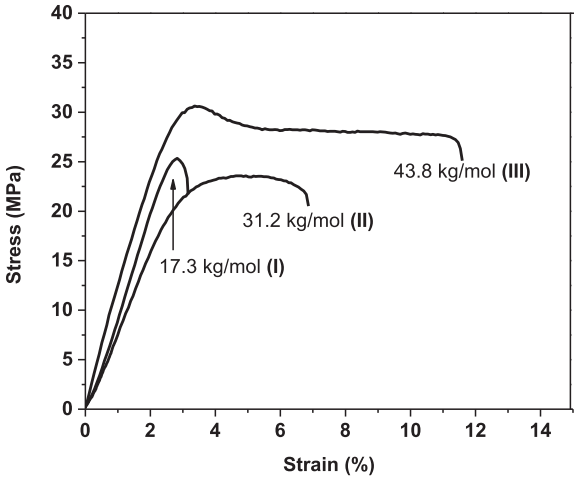

Fig. 2. Characteristic stress–strain curves obtained from the compression molded polymers **I**, **II** and **III**.

From Fig. 3, it can be seen that no rubber plateau region is detected for either G′ or G″ up to 260 °C. Instead, the G′ and G″ decrease with decreasing angular frequency (ω) indicating that the measurements are performed in the terminal regime. The absence of a rubber plateau is commonly observed during frequency sweeps of semi-flexible thermotropic polyesters [21–23].

It is noticed that above 200 °C the data points of G′ start to scatter at low ω values (<1 rad/s). It is thought that the scattering in the data is a result of the G′ values being too close to the transducer limits. However, it can be clearly seen that the decay of G′ slowly levels off at low angular frequencies for measurements performed between 170 °C and 200 °C. Similarly the slope of the log G″ versus log G′ plots does not follow the characteristic slope value of two, expected for liquid-crystalline polymers in the isotropic phase as shown in Fig. 4 [22,24,25]. Instead, an enhanced storage modulus is observed at low values, characteristic for the nematic phase. As is reported by Zhou and coworkers, this long relaxation tail at low oscillatory frequencies is a result of distortional elasticity related to the defect structure of the nematic phase [21]. Thus the data in Fig. 4 clearly indicates that polymer **III** resides in a full nematic phase below 200 °C.

As is visible from Fig. 3a, the relaxation tail at low oscillatory frequencies seems to diminish slowly at higher temperatures, indicating that a slow or partial transition from the nematic to isotropic (N–I) phase might be occurring. This data is in contrast to our observations in polarization optical microscopy, where no isotropic phase is detected below degradation occurring close to

Table 1
Molecular weights, thermal properties and mechanical performance of compression molded polymers **I**–**III**.

Entry	SEC		DSC		DMTA	Tensile testing		
	M_w (kg/mol)	PDI (–)	T_g (°C)	T_m[a] (°C)	T_g (°C)	E (GPa)	σ_{max} (MPa)	ε_{break} (%)
I	17.3	2.14	43.1	125.9	50.8	0.96 (0.13)	23.1 (2.88)	4.14 (2.17)
II	31.2	2.40	44.6	126.7	51.0	0.90 (0.05)	20.7 (2.21)	6.38 (0.85)
III	43.8	2.56	45.7	127.1	51.7	1.09 (0.12)	29.7 (2.49)	12.55 (0.35)

[a] T_m in this study is defined as the crystal to nematic phase (K–N) transition. In the polymers synthesized in this study, no nematic to isotropic transition is detected in cross-polarization optical microscopy upon continuous heating of the polymers **I**–**III**. Standard deviations in the measured values of the tensile properties, taken from ten samples, are given in brackets.

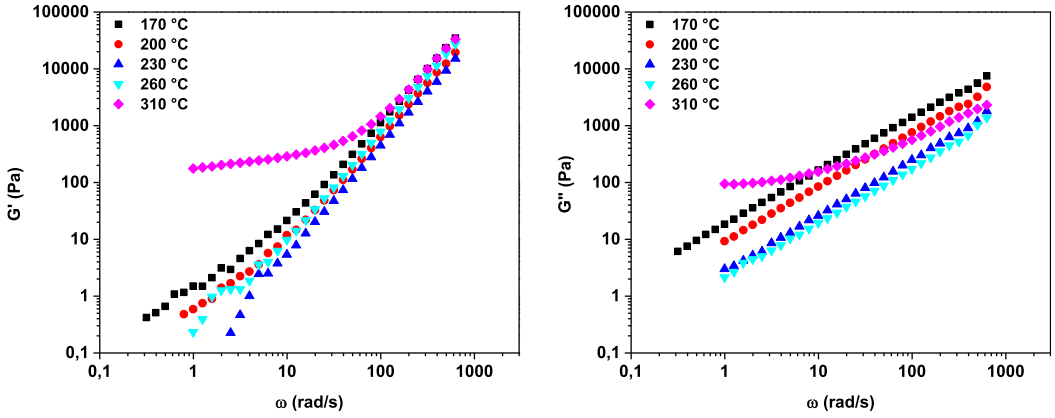

Fig. 3. Elastic modulus G′ (left) and viscous modulus G″ (right) observed during rheology experiments of polymer **III** as a function of angular frequency ω performed at temperatures varying from 170 °C to 310 °C.

300 °C. The rheological response of polymer **III** changes significantly at 300 °C or higher. A plateau value for both G′ and G″ is observed at low ω values, indicating that the polymer cross-links at the high temperature.

Overall, from the rheological data it is concluded that processing of polymer **III** from the nematic melt should be performed below 200 °C.

3.2. Extrusion and melt-drawing of the thermotropic polyesters

Small scale melt-drawing experiments were performed at 170 °C using a twin-screw extruder, since a good overall spinnability was observed for polymers **I**–**III** at this temperature. Once extruded, the strand was quenched in a water bath and wound on a bobbin. The draw ratio was controlled by a variation of the winding speed. To ensure a high orientation of the fibers, the water bath was placed at 1 cm distance from the extruder outlet. Since the fiber is quenched once it touches the water surface, the drawing process takes place over the 1 cm in-between the extruder outlet and the water bath. The average draw ratio of the obtained fibers is calculated by dividing the cut-through area of the obtained fiber by the area of the extruder outlet. The diameter of the fiber was calculated using the length and mass of the obtained fiber and the density (1.21 g/cm^3) of the non-oriented polymer.

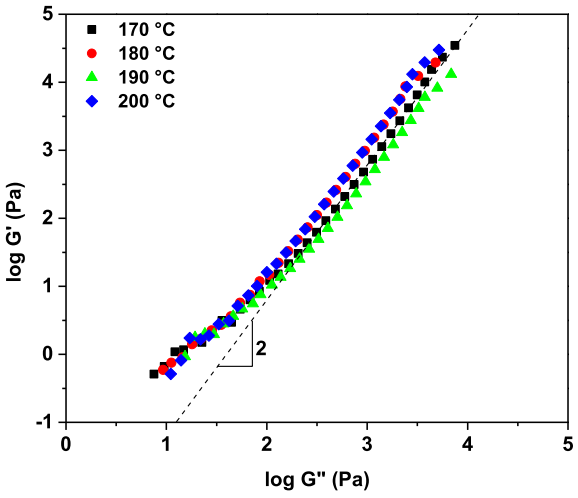

Fig. 4. G″ versus G′ plotted for frequency sweeps performed on polymer **III** at temperatures between 170 °C and 200 °C. It can be seen that the expected slope of 2 in the log G″ versus log G′ plot, characteristic for isotropic materials, is not followed at low moduli.

The fibers obtained after spinning polymer **I** could not be wound, since they were too brittle and broke during the winding process. This indicates that the molecular weight of this polymer it too low for uniaxial deformation. In contrast, polymers **II** and **III** could be easily spun at these conditions and were wound at varying draw ratios. Fig. 5a shows an overview of the storage modulus (E′) of the fibers of polymers **II** and **III** as a function of the draw ratio, obtained after DMTA analysis. Fig. 5b shows the Young's modulus of the fibers of polymer **III** as determined via tensile testing. For comparison, the storage modulus observed in DMTA is added in Fig. 5b.

As is clearly visible in Fig. 5a, the modulus of the fibers made from both polymers increases with the draw ratio. Furthermore, fibers of polymer **III** exhibit higher storage moduli than polymer **II** when processed at the same conditions and draw ratio. This is probably a result from the difference in relaxation times of the oriented polymer chains prior to quenching in the water bath. As is suggested by Jackson and coworkers, processing of a thermotropic hydroxybenzoic acid and poly(ethylene terephthalate) based copolymer at increasing temperatures yields products with lower modulus, due to a faster relaxation of the polymers prior to quenching [26]. Similarly, the relaxation of polymer chains is also dependent on molecular weight, since relaxation and chain dynamics of short polymer chains is generally faster than in long polymer chains. For this reason, we anticipate that the slower relaxation during processing of polymer **III** facilitates higher storage modulus.

Since the fibers spun from polymer **III** show better performance, tensile tests were performed on these fibers. In general, it is observed that fibers with a high draw-ratio exhibit a lower strain at break. Furthermore, it is observed that the stress at break of the fibers increase with increasing draw-ratio. This becomes evident when the tensile stress is plotted as a function of draw ratio for fibers that break between 2.5% and 3.5% strain (Fig. 6).

The fibers spun from polymer **III** were characterized using 2D wide-angle x-ray diffraction (WAXD) and their order parameter $\langle P_{2n}(\cos\varphi)\rangle_d$ was determined (Fig. 7). The order parameter $\langle P_{2n}(\cos\varphi)\rangle_d$ is determined from an average of a Legendre polynomial, weighted against the obtained azimuthal intensity scan as described in the experimental section. Fig. 7a shows a characteristic 2D-WAXD fiber pattern and the corresponding azimuthal intensity scan taken at the maximum of the inter-chain diffraction peak at $2\theta = 21°$. Fig. 7b shows the obtained orientation parameters $\langle P_{2n}(\cos\varphi)\rangle_d$ for fibers of polymer **III**, with varying draw ratios. In

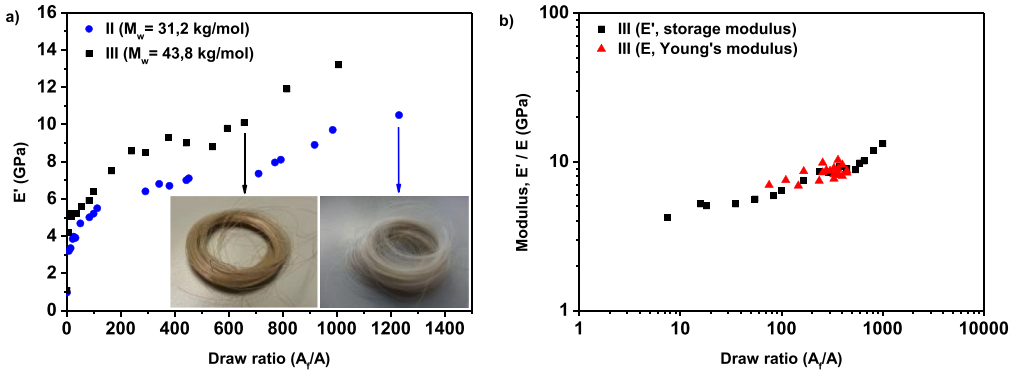

Fig. 5. a) Storage modulus (E′) versus draw ratio plot as observed in DMTA analysis for fibers spun from polymers **II** and **III**. Figures of the obtained fibers after continuous spinning are enclosed. b) Young's modulus as a function of the draw ratio of spun fibers from polymer **III** as determined via tensile testing. The experimental data points, shown in the figure, were obtained at room temperature.

general, it can be seen that an increase of the draw ratio results in an increase of the orientation parameter. These results are in good agreement with the continuous increase of the storage/tensile modulus and the tensile strength of the fibers, which all increase with the draw-ratio. These data therefore suggest that a strong alignment and mechanical performance of these aliphatic-aromatic fibers is only obtained at high draw-ratios. Such a strong dependency of the mechanical performance on the draw-ratio was also observed by Acierno and coworkers, during the spinning experiments of the PET/BA based thermotropic copolymers (60 mol% BA) at varying draw ratios and temperatures [11].

In general, these preliminary single-filament fiber spinning experiments show that these vanillic acid based thermotropic polyesters can easily be spun from the melt and that their modulus, tensile strength, and orientation can be improved by increasing the draw ratio. Using the procedure reported in this study, fibers having tensile modulus >10 GPa and a tensile strength >150 MPa can be easily spun from polymer **III**. FTIR and solid-state NMR experiments indicate that only the aromatic components are molecularly oriented during the spinning process (Supporting Information). In contrast, the aliphatic moieties exhibit a high mobility, normally corresponding to a local isotropic motion. It is expected that the poor molecular orientation of the aliphatic moieties in these aliphatic-aromatic thermotropic polyester contribute to the relatively low tensile modulus of the fibers, obtained after the extrusion and melt-drawing process.

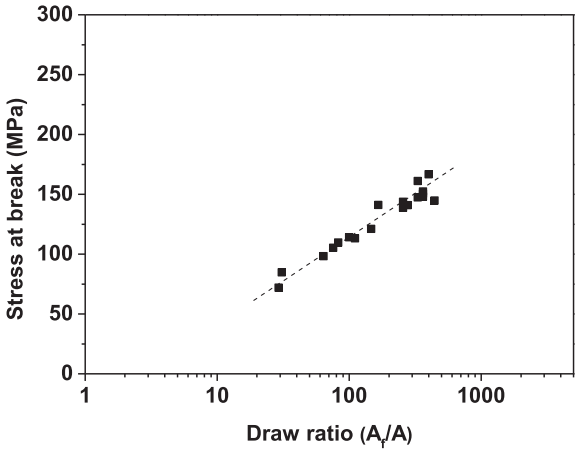

Fig. 6. Stress at break versus draw ratio observed in tensile testing of spun fibers of polymer **III**, having a strain at break between 2.5 and 3.5%. The dotted line is added to guide the eye.

Furthermore, although the obtained values are promising, as is reported by Muramatsu and coworkers [27], optimization of the spinning procedure should be performed by controlling the processing temperature, the extrusion velocity, and the winding speed/draw ratio. It should be noted that generally it is advisable to place a die at the extruder outlet to promote pre-orientation of the melt and to facilitate higher draw-ratio and orientation in of the fibers after the spinning process. However, preliminary spinning results using a die with an internal draw ratio of 36 (d_{in} = 6 mm, d_{out} = 1 mm) did not seem to affect the properties of the fibers obtained after the melt-drawing process. For this reason, no further optimization of the spinning process was pursued.

3.3. *Effect of orientation on the thermal properties*

In the previous section we have demonstrated that fibers can be readily spun from the thermotropic melt. The fibers obtained after spinning were characterized using DSC and DMTA analysis. Fig. 8 shows an overview of the first heating run in the DSC analysis performed at 10 °C/min of the compression molded sample, the as-spun fiber and the fiber after annealing at 100 °C for 24 h. It can be clearly seen that the melt-drawing process does not influence the melting behavior of the polymer, as is indicated by the comparable enthalpy of the melting observed at 126 °C for the compression molded sample (1.94 J/g) and the as spun fiber (2.08 J/g). This indicates that the crystallinity of the compression molded and the spun fibers are comparable. Although no changes in melting behavior are observed upon fiber spinning, the performance of a heat-treatment (HT) results in a slight increase in melt-enthalpy indicating a slightly higher crystallinity of the fiber after annealing at 100 °C.

WAXD analysis was employed to identify the changes in crystallinity as a function of processing and annealing. In order to calculate the crystallinity, peak fitting of the inter-chain diffraction peak and the amorphous scattering was performed and the crystallinity was obtained by dividing the area of the diffraction peak at $2\theta = 21°$ by the total area of the diffractogram. Following this procedure, a crystallinity of 31% is calculated for the compression molded sample of polymer **III**. In contrast, the heat-treated fibers show a crystallinity of ~70–73%.

As is visible from the 2D WAXD fiber diffractogram inset in Fig. 7a, there are no strong diffraction peaks in the diffractogram other than the inter-chain diffraction peak. It should be noted that a weak diffraction signal is observed at $2\theta \sim 8–9°$ (inset of Fig. 7a), likely corresponding to the diffraction originating from the suberic acid spacer. However, the intensity of this signal is very low and can

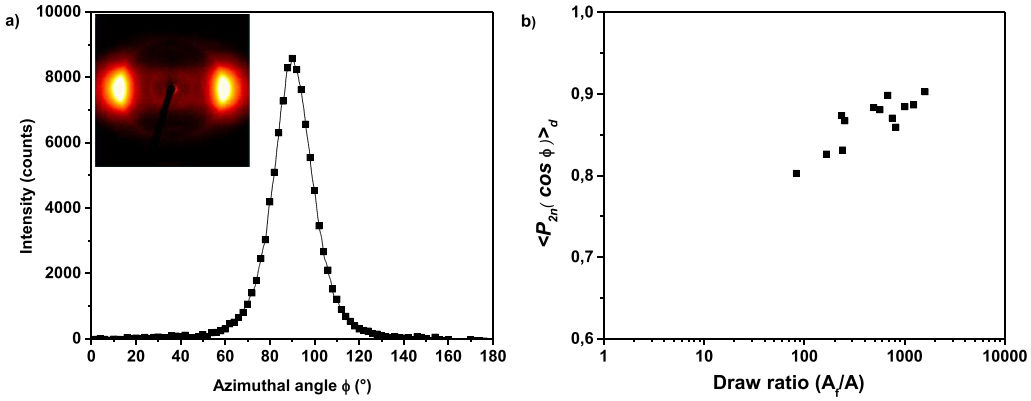

Fig. 7. a) Characteristic WAXD pattern of the fibers developed in this study and the azimuthal density distribution of the oriented diffraction peak corresponding to the inter-chain distance taken at $2\theta = 21^{\circ}$ and, b) Order parameter $<P_{2n}(\cos\varphi)>_d$ as a function of draw ratio for fibers of polymer **III**.

therefore not be used to differentiate between the oriented amorphous fraction and the crystalline fraction in the fibers using WAXD analysis [28]. Nonetheless, when the results from WAXD and DSC analysis are combined, it can be concluded that fiber spinning results in a strong orientation of the amorphous phase, whereas annealing results in a significant increase of the crystallinity of the sample evident from the increase in melt enthalpy to 5.54 J/g from 2.08 J/g (Fig. 8).

According to DSC analysis, the glass transition of the spun polymers is not strongly influenced by the orientation of the fibers; the T_g of both the compression molded samples and the fibers lie in the range between 45 and 48 °C. As is clearly visible from Fig. 8, the as spun fiber exhibits a strong endotherm above T_g. This is thought to be a result of the release of stresses induced by the quenching step in the spinning process. In contrast to the DSC analysis, a clear increase of the glass transition temperature is observed for the oriented fibers when the thermal behavior is evaluated by DMTA analysis. As is visible from Fig. 9, the peak in the loss modulus (E″), characteristic for the glass transition, increases by roughly 10 °C for the oriented and annealed sample (60.7 °C) compared to the compression molded sample (51.7 °C). Similarly, the T_g of the as spun fibers increases by 3–10 °C compared to the compression molded samples, depending on the applied draw-ratio of the fiber. This data clearly shows that, although not detectable in DSC analysis, an increased orientation of the polymer chains causes an increase of the glass transition temperature.

Fig. 10 shows the dependence of the orientation parameter $<P_{2n}(\cos\varphi)>_d$ of a fiber with a draw ratio of 100 as a function of temperature (heating rate of 10 °C/min). For comparison, the first DSC heating trace of the same fiber is added. From Fig. 10 it can be seen that the fiber relaxes slowly upon heating, resulting in a slight decrease of the orientation. For example, the fiber has an orientation parameter of 0.81 at 20 °C and the orientation parameter decreases to 0.79 upon heating to 100 °C. Upon further heating, melting starts to occur and a rapid loss of the orientation occurs. To illustrate this, an orientation parameter of 0.45 is found at 150 °C, indicating that the sample is fully molten and resides in a slightly ordered liquid crystalline melt.

It is clear from the thermal characterization of the fibers that, although these fibers retain their orientation above their glass transition, as anticipated, loss of the orientation occurs rapidly upon melting. This data implies that these fibers cannot be used at temperatures well above 100 °C. Furthermore, as is reported in the previous sections, a high temperature heat-treatment normally results in an increase of the molecular weight and crystallization by reorganization. As a result, the fibers subjected to such an annealing step generally exhibit higher melting temperatures, which in turn allows for their application at higher temperatures. Unfortunately, as is shown by DSC and WAXD analysis, the application of a heat-treatment step at temperatures below the melting

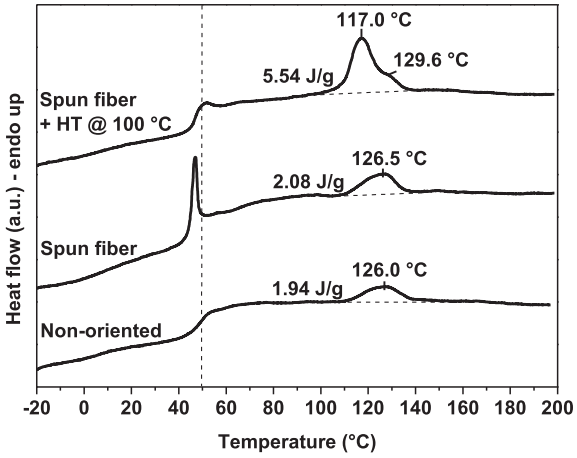

Fig. 8. DSC heating runs of polymer **III** performed at 10 °C in the non-oriented state, the as-spun fiber, and the spun fiber after annealing for 24 h at 100 °C (spun fiber + HT @ 100 °C). For the DSC experiments, a bundle of fibers having a draw ratio of 1500 was used.

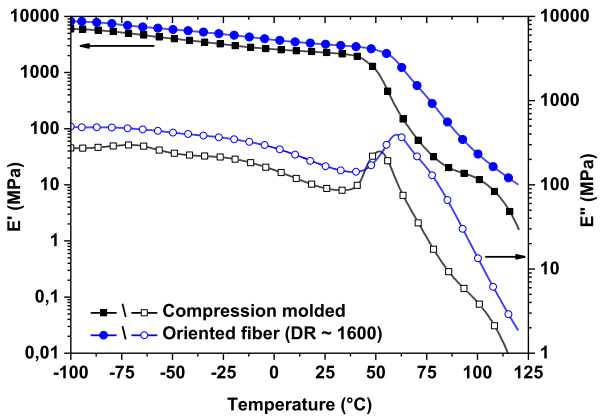

Fig. 9. Temperature dependence of the storage (E′) and loss (E″) moduli for the compression molded polymer **III** and a bundle of oriented fibers with an average draw-ratio of 1500.

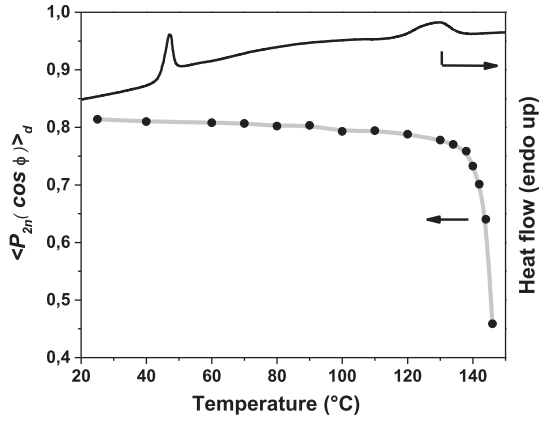

Fig. 10. Orientation parameter $<P_{2n}(\cos\varphi)>_d$ versus temperature plot, in combination with the first DSC heating run of the same fiber (DR = 100). Both experiments were performed at a heating rate of 10 °C/min.

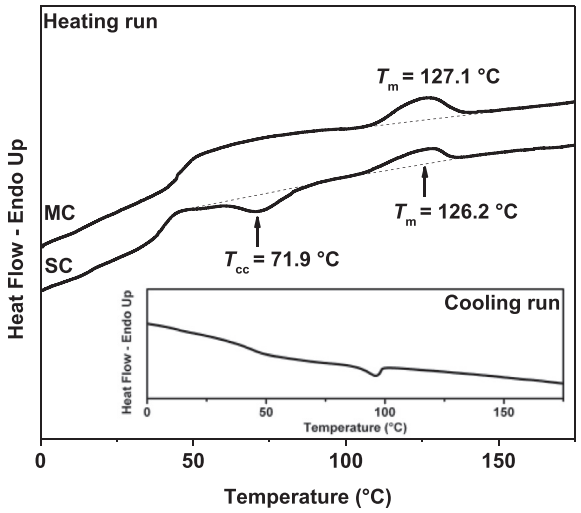

Fig. 12. DSC heating run of a dried solvent-cast film (SC) and melt-crystallized film (MC) performed at a heating rate of 10 °C/min. The DSC trace observed during cooling at a rate of 10 °C/min identical for the MC and SC samples. For this reason, only the cooling run of the SC film is embedded on the bottom of the figure.

temperature of the fibers developed in this study does not significantly influence the melting temperature.

3.4. Solvent casting for film preparation

In order to investigate the effect of solvent based processing techniques on the mechanical properties, solvent cast films were prepared following the procedure reported in the experimental section. After drying the samples at 40 °C, overnight *in vacuo*, the obtained films of polymers **I** and **II** were extremely brittle and could not be used for mechanical testing. For polymer **I** this indicates, similar to our observations of the melt processed products of this polymer, that the molecular weight is too low for processing. The brittle behavior of polymer **II** was unexpected since this polymer can easily be processed from the melt and yields highly oriented fibers. In contrast, polymer **III** could easily be solvent cast to form transparent films. As is shown in Fig. 11, these films show no birefringence in polarized optical microscopy, indicating that they do not reside in the nematic liquid crystalline phase (Fig. 11, 50 °C). The absence of the birefringence indicates that these films reside either in an amorphous or in a homeotropic liquid crystalline phase. However, DMTA analysis shows a plateau for the E′ modulus above T_g indicating that these films are, in fact, semi-crystalline. The absence of the birefringence in the semi-crystalline film suggests the presence of some short range order that can be perpendicular or parallel to the dried films, of the high molar mass polymer **III**. As is visible from the micrograph taken at 90 °C in Fig. 11, heating above the glass transition results in a further crystallization of the sample. This cold-crystallization behavior is confirmed by DSC analysis, as is shown in the heating trace of the solvent cast (SC) sample and the melt-crystallized (MC) samples, obtained at a heating rate of 10 °C (Fig. 12). Further heating of the solvent cast film results in melting of the crystals and a slow reorganization of the polymer chains into the liquid crystalline melt, as is shown in Fig. 11 for the micrographs taken at 120 °C and higher. On heating (10 °C/min) and subsequent fast cooling (50 °C/min) of the solvent-cast films from the liquid crystalline state to room temperature, results into a supercooled liquid crystalline glass (nematic glass).

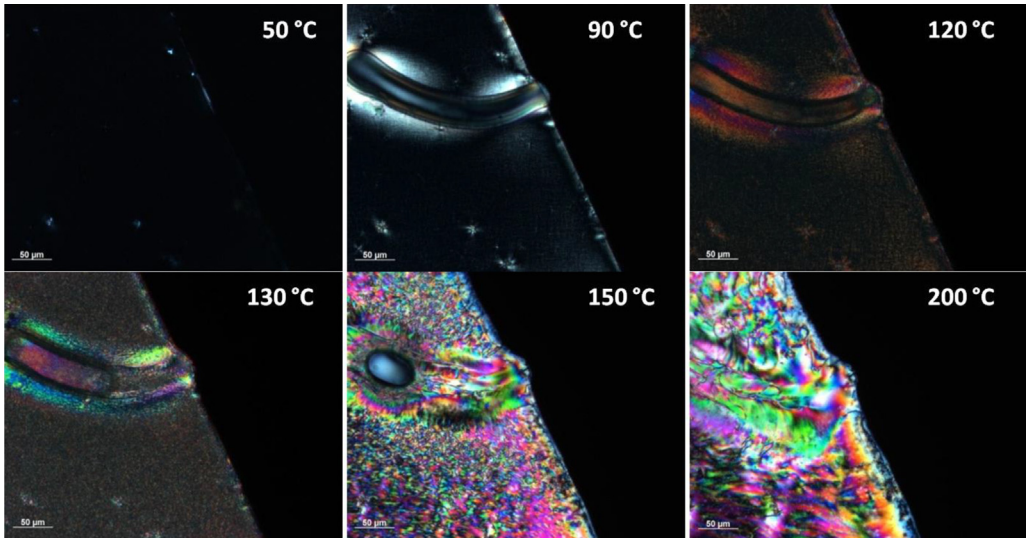

Fig. 11. Optical micrographs taken between cross-polars during heating a solvent cast film of the polymer **III**, at 10 °C/min. The polymer film does not show birefringence and stays transparent below T_g. The film goes through cold-crystallization above T_g, and transforms into a nematic phase at higher temperatures.

Table 2
Effect of processing method on the tensile performance of polymer **III**.

Processing method	Tensile performance		
	E (GPa)	σ_{max} (MPa)	ε_{break} (%)
Solvent casting	0.11 (0.02)	9.69 (1.12)	114.5 (14.7)
Solvent casting + HT	0.81 (0.05)	29.7 (0.94)	14.4 (1.45)
Compression molding	1.09 (0.12)	29.7 (2.49)	12.6 (0.35)
Fiber spinning[a]	8.75 (0.77)	157 (32.5)	2.46 (0.83)

[a] The draw ratio of the fibers reported in this table was 400.

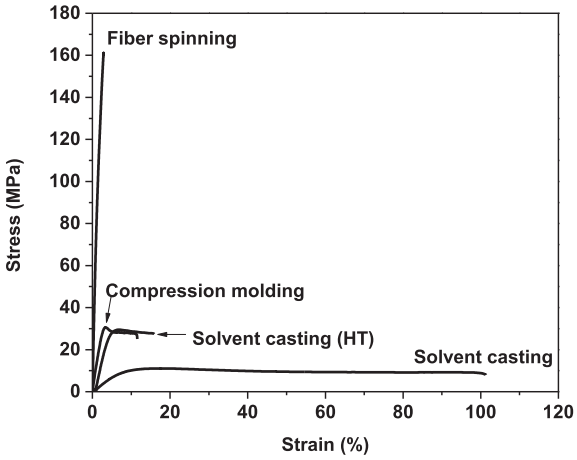

Fig. 13. Characteristic stress–strain curves of the products obtained after processing of the polymer **III** through fiber spinning, compression molding or solvent casting. The latter is investigated before and after annealing, where the annealing was performed at 80 °C for 12 h.

Although the very thin films prepared for polarized optical microscopy and DSC analysis were easily dried and contained no residual solvent, it was noticed that thick films prepared for mechanical testing contained some solvent after drying at 40 °C *in vacuo*. It is likely that this solvent is trapped during the drying process that is performed below T_g of the polymer. Therefore, to ensure that the polymer is thoroughly dried prior to the performance of mechanical tests, the solvent cast films were dried *in vacuo* at 80 °C overnight. Next, the tensile performance of the solvent cast films dried at 40 °C and 80 °C was evaluated. The solvent cast films dried at 40 °C were ductile and could be elongated more than 100% prior to failure. Since the modulus (~0.1 GPa) and yield point (~10 MPa) of these films are low it can be concluded that the residual solvent acts as a plasticizer, limiting the crystallization and improving the elongation at break. In contrast, the samples dried at 80 °C showed a tensile behavior very similar to the compression molded samples. The observed tensile modulus, stress at break and strain at break were 0.81 GPa, 29.7 MPa and 14.4% respectively, indicating that crystallization increases the stiffness, but also the brittle behavior of the sample. Such a brittle behavior is characteristic for aliphatic-aromatic semi-crystalline polyesters such as poly(butylene terephthalate). Table 2 summarizes the tensile performance of products obtained after processing of polymer **III** using the various methods evaluated in this study, including the solvent cast films. Similarly, Fig. 13 gives an overview of the characteristic stress–strain curves observed for the products listed in Table 2.

4. Conclusions

In this study we have addressed melt drawing, compression molding and solvent casting of aromatic-aliphatic thermotropic polyesters based on vanillic acid. It is observed that these polymers require a M_w of at least 30 kg/mol to be successfully drawn and wound from the melt during fiber spinning. In general, an increase of the orientation, tensile modulus and tensile strength is observed with increasing molar mass and draw ratio of the fiber. Although fiber spinning is easily achieved at 170 °C and highly oriented fibers can be obtained, it is observed that these fibers are only dimensionally stable up to ~120–130 °C. Above this temperature, melting starts to occur and the orientation of the samples is slowly lost. In general, this implies that these fibers cannot be used for demanding applications where high temperatures are required. Nonetheless, the developed concepts demonstrate that a random distribution of the monomer along the polymer chains facilitates ease in deformation and provides better properties than when the monomers are alternatingly present in the polymer backbone, as is reported by Krigbaum and coworkers [27]. In order to develop fully renewable thermotropic polyesters with high temperature resistance, it is advised to decrease or eliminate the aliphatic content in the polymer backbone. Such a decrease of the aliphatic content results in longer relaxation times of the polymer during processing, most likely yielding fibers with better mechanical performance. Furthermore, a decrease of the aliphatic content allows for the development of thermotropic polymers with higher melting temperatures that can be submitted to a high-temperature heat-treatment step, which will further enhance their properties.

Acknowledgements

This work is part of the research program of the Dutch Polymer Institute (DPI), #739 BioLCP.

Appendix A. Supplementary data

Supplementary data related to this article can be found at http://dx.doi.org/10.1016/j.polymer.2015.01.045.

References

[1] Han H, Bhowmik PK. Prog Polym Sci 1997;22:1431–502.
[2] Ballauff M. Angew Chem 1989;101:261–76.
[3] Windle AH. In: Shibaev VP, Lam LM, editors. Liquid crystalline and mesomorphic polymers. New York: Springer-Verlag; 1994 [Chapter 2].
[4] Lin J, Sherrington DC. Adv Polym Sci 1994;111:177–219.
[5] Varshney SK. J Macromol Sci Rev Macromol Chem Phys 1986;C26(4):551.
[6] Dobb MG, McIntyre JE. Adv Polym Sci 1984;60/61:61–98.
[7] Chung T-S. Polym Eng Sci 1986;26(13):901–19.
[8] Jackson Jr WR. Mol Cryst Liq Cryst 1989;169:23–49.
[9] Warner SB, Lee J. J Polym Sci Part B: Polym Phys 1994;32:1759–69.
[10] Grasser W, Schmidt H-W, Giesa R. Polymer 2001;42:8529–40.
[11] Acierno D, La Mantia FP, Polizzotti G. Macromolecules 1982;15:1455–60.
[12] Econ J Mol Cryst Liq Cryst 1989;169:1–22.
[13] De Ruijter C, Bos J, Boerstoel H, Dingemans T. J Polym Sci Part A: Polym Chem 2008;46:6565–74.
[14] Wilsens CHRM, Noordover BAJ, Rastogi S. Polymer 2014;55(10):2432–9.
[15] Wilsens CHRM, Verhoeven JMGA, Noordover BAJ, Hansen MR, Auhl D, Rastogi S. Macromolecules 2014;47(10):3306–16.
[16] Li XG, Huang MR. Polym Plast Technol Eng 2000;39(2):317–31.
[17] Li XG, Huang MR, Guan G-H, Sun T. J Appl Polym Sci 1997;66:2129–38.
[18] Nagata M. J Appl Polym Sci 2000;78:2474–81.
[19] Mitchell GR, Windle AH. In: Basset DC, editor. Developments in crystalline polymers, chapter 3: orientation in liquid crystal polymers – 2. London, UK: Elsevier Applied Science Publishers LTD; 1988.
[20] Ugaz V, Burghardt WR, Zhou W, Kornfield JA. J Rheol 2001;45:1029–63.
[21] Zhou W-J, Kornfield JA, Ugaz V, Burghardt WR, Link D, Clark NA. Macromolecules 1991;32:5581–93.
[22] Kim SS, Han CD. Macromolecules 1993;26:6633–42.
[23] Somma E, Nobile MR. J Rheol 2004;48(1407):1422.
[24] Kim SS, Han CD. J Rheol 1993;37:847–66.
[25] Zhou M, Han CD. Macromolecules 2006;39:232–42.
[26] Jackson WJ, Kuhfuss HF. J Polym Sci Polym Chem Ed 1976;14:2043–58.
[27] Muramatsu H, Krigbaum WR. J Polym Sci Part B: Polym Phys 1986;24:1695–711.
[28] Karacan I. J Appl Polym Sci 2006;100:142–60.